Optimum control system for earthquake-excited building structures with minimal number of actuators and sensors

Jia He[*], You-Lin Xu, Chao-Dong Zhang and Xiao-Hua Zhang

Department of Civil and Environmental Engineering, The Hong Kong Polytechnic University, China

Abstract. For vibration control of civil structures, especially large civil structures, one of the important issues is how to place a minimal number of actuators and sensors at their respective optimal locations to achieve the predetermined control performance. In this paper, a methodology is presented for the determination of the minimal number and optimal location of actuators and sensors for vibration control of building structures under earthquake excitation. In the proposed methodology, the number and location of the actuators are first determined in terms of the sequence of performance index increments and the predetermined control performance. A multi-scale response reconstruction method is then extended to the controlled building structure for the determination of the minimal number and optimal placement of sensors with the objective that the reconstructed structural responses can be used as feedbacks for the vibration control while the predetermined control performance can be maintained. The feasibility and accuracy of the proposed methodology are finally investigated numerically through a 20-story shear building structure under the El-Centro ground excitation and the Kobe ground excitation. The numerical results show that with the limited number of sensors and actuators at their optimal locations, the predetermined control performance of the building structure can be achieved.

1. Introduction

In the past few decades, considerable attention has been paid to structural vibration control technology for sustaining the safety and serviceability of civil structures against strong winds, earthquakes and other natural or man-made hazards (Housner *et al.* 1997, Spencer and Nagarajaiah 2003, Xu and Ng 2008, Fisco and Adeli 2011). Many real implementations of vibration control technology have also been realized throughout the world (Aupérin *et al.* 2001, Soong and Spencer 2002, Ikeda 2009). For active or hybrid control technology, the vibration control system mainly comprises two interacted parts: sensory system and actuator system. One of the important issues is how to place a minimal number of actuators and sensors at their respective optimal locations to achieve the predetermined control performance. This issue is particularly important for large civil structures because of their huge sizes and complex structural systems. However, in the field of civil engineering the research on the optimal placement of sensors often refers to structural

---

∗Corresponding author, Ph.D., E-mail: hj19830507@gmail.com

damage detection whereas the study on the optimal placement of actuators always makes reference to structural vibration control (Rao and Anandakumar 2008, Yi *et al.* 2012, Bigdelia *et al.* 2012). Unlike the mechanical and aerospace engineering arena, combinatorial optimization methods as a means for identifying sets of actuators and sensors that maximize control performance are limited for civil structures.

To provide maximum information on the state of a structure, numerous methods have been developed for solving the optimal sensor placement problem. For example, Kammer (1991) proposed a method, termed Effective Independence (EfI) method, to optimize sensor locations based on the contribution of each sensor location to the linear independence of the identified modes. Based on the Fisher information matrix, Udwadia (1994) proposed a methodology for the optimal sensor location in such a way that the measurements obtained from those locations are most informative about the estimated parameters. Heo *et al.* (1997) suggested an optimal sensor placement method based on the maximization of modal kinetic energy. Its objective is to find a reduced sensor configuration which maximizes the measure of the kinetic energy of a structure. The inherent mathematical connection between the EfI and kinetic energy methods was revealed by Li *et al.* (2007). More recently, Zhang *et al.* (2011, 2012) proposed a sensor placement approach for the optimal configuration of multi-type sensors to achieve the best multi-scale response reconstruction for monitoring a structure. A comprehensive review on the optimal sensor placement has been provided by Barthorpe and Worden (2009).

For the optimal placement of control devices, extensive studies have also been performed. Some investigations were carried out to find optimal configuration of control devices by minimizing the amplitude of transfer functions evaluated at the fundamental frequency (Takewaki 1997, 2000, Aydin *et al.* 2007). Another type of widely used objective function for optimizing controller placement is based on the minimization of building performance indices in the time domain (Zhang and Soong 1992, Liu *et al.* 2005, Whittle *et al.* 2012) or on the properties of the control system or control law such as the controllability (Hac and Liu 1993, Peng *et al.* 2005). Based on the linear quadratic performance index, a relatively simple increment algorithm was also proposed by Xu and Teng (2002) for the optimal placement of control devices for building structures under earthquake excitations.

In the field of mechanical and aerospace engineering, the optimal configuration of the actuators and sensors are often simultaneously considered primarily due to the meticulous requirement of control effectiveness and the wide application of smart materials such as piezoelectric ceramics or shape memory alloys. Comprehensive reviews on this topic can be found in the literatures (Frecker 2003, Gupta *et al.* 2010). However, combinatorial optimization methods for identifying locations of both actuators and sensors for vibration control of civil structures are relatively limited. In this paper, a relatively simple and cost-effective method is presented for the determination of the minimal number and optimal location of actuators and sensors for vibration control of building structures under earthquake excitation. In the proposed method, the number and location of the actuators are first determined in terms of the sequence of performance index increments and the predetermined control performance. A multi-scale response reconstruction method is then extended to the controlled building structure for the determination of the minimal number and optimal placement of sensors with the objective that the reconstructed structural responses can be used as feedbacks for the vibration control while the predetermined control performance can be maintained. The feasibility and accuracy of the proposed methodology are finally investigated numerically through a 20-story shear building structure under the El-Centro ground excitation and the Kobe ground excitation.

2. Increment-based approach for optimal placement of actuators

It is well known that the equation of motion of a controlled building structure of multi-degrees of freedom (MDOFs) under earthquake excitation can be given by

$$[M]\{\ddot{x}\}+[C]\{\dot{x}\}+[K]\{x\}=-[M]\{1\}\ddot{x}_g+[H_c]\{U\} \tag{1}$$

in which $x, \dot{x}$ and $\ddot{x}$ are respectively the displacement, velocity, and acceleration response vector; $[M]$, $[K]$ and $[C]$ are respectively the mass, stiffness and damping matrix of the building structure; $\{U\}$ is the control force vector; $[H_c]$ is the matrix denoting the location of the control force; and $\ddot{x}_g$ is the ground acceleration. Eq. (1) can also be converted to the following continuous state-space equation.

$$\{\dot{X}\}=[A_c]\{X\}+[B_c]\ddot{x}_g+[D_c]\{U\} \tag{2}$$

where

$$\{X\}=\begin{bmatrix}\{x\} & \{\dot{x}\}\end{bmatrix}^T \tag{3}$$

$$[A_c]=\begin{bmatrix}[0] & [I] \\ -[M]^{-1}[K] & -[M]^{-1}[C]\end{bmatrix};[B_c]=\begin{bmatrix}\{0\} \\ -\{1\}\end{bmatrix};[D_c]=\begin{bmatrix}[0] \\ [M]^{-1}[H_c]\end{bmatrix} \tag{4}$$

The following linear quadratic performance index is often used for vibration control of a building structure under random disturbance.

$$J=\frac{1}{2}E\left\{\int_0^{t_f}\left(\{X\}^T[Q]\{X\}+\{U\}^T[R]\{U\}\right)dt\right\} \tag{5}$$

where $[Q]$ and $[R]$ are the weighting matrices for the structural response and control force, respectively; E is the expectation operator; and t_f is the duration defined to be longer than that of the earthquake. For a close-loop control configuration with the ground motion being a white noise random process, minimizing Eq. (5) subject to the constraint of Eq. (2) results in the following optimal control force vector

$$\{U\}=-[G]\{X\} \tag{6}$$

where $[G]$ is the control gain given by

$$[G]=[R]^{-1}[D_c]^T[P] \tag{7}$$

The matrix $[P]$ is the solution of the following classical Riccati equation.

$$[A_c]^T[P]+[P][A_c]-[P][D_c][R]^{-1}[D_c]^T[P]+[Q]=0 \tag{8}$$

The increment of the performance index for the optimal location of control device is given by

$$\Delta J_i = -tr\left\{\left([\bar{X}_0]+[F]\right)[S][\Delta D_c]_i[G]\right\} \quad (i=1, 2,\ldots,j) \tag{9}$$

where

$$[\bar{X}_0] = \{X\}_0\{X\}_0^T \tag{10}$$

$$[F] = E\left\{\int_0^{t_f} \{[B_c]\ddot{x}_g(\tau)\}\{[B_c]\ddot{x}_g(\tau)\}^T d\tau\right\} \tag{11}$$

$$[S] = \int_0^{t_f} t[\chi(t)]^T[\bar{Q}][\chi(t)]dt \tag{12}$$

$$[\chi(t)] = \exp\{([A_c]-[D_c][G])t\} \tag{13}$$

$$[\bar{Q}] = [Q]+[G]^T[R][G] \tag{14}$$

in which ΔJ_i and $[\Delta D_c]_i$ denote respectively the increment of the performance index and the change of the position matrix of control devices $[D_c]$ when the i-th control device is removed; j is the number of the removed control devices; and $\{X\}_0$ denotes the initial state of the structure.

The increment of the optimal performance index due to the removal of the i-th control device, calculated by Eq. (9), reflects the sensitivity of the i-th control device to the performance index. A small increment of the index means a low sensitivity and less importance of the i-th control device to the total control performance whereas a high increment implies that the i-th control device has great influence on the total control performance. Therefore, based on the calculated increments from the removal of each control device, the sequence of importance of all the control devices can be obtained. For the sake of easy comparison, a contribution percentage (*CP*) index is presented and defined as follows

$$CP_i = \frac{\Delta J_i}{\sum_{i=1}^{j} \Delta J_i} \tag{15}$$

It can be seen from Eq. (15) that the larger value of the CP_i indicates the more important influence of the i-th control device on the total control performance. Consequently, this index provides great convenience for determining the number and placement of control devices according to the predetermined control performance. Moreover, different from the classical integer heuristic programming methods such as the sequential search algorithm (SSA) (Zhang and Soong 1992) or the Worst-Out-Best-In (WOBI) algorithm (Haftka and Adelman 1985), the actuator placement method basing on the sequence of the calculated CP_i in this study is relatively simple and time-saving because the value of CP_i does not need to re-evaluated when other actuator is removed. The comparative results of these methods will be shown and discussed in the subsequent numerical example in details.

Since the number and location of the actuators are determined according to the sequence of the CP_i, the structural vibration could be controlled by the determined actuators using the response measurements as the feedbacks. However, it is usually difficult to install enough sensors to obtain the complete structural responses for vibration control of a large civil structure. Consequently, for

the purpose of the cost-saving and potential application to real structures, the aforementioned control system with the optimal location of the actuators should be improved by the combination of some other technologies which can provide the complete structural responses for vibration control using the limited observations.

3. Response reconstruction-based approach for optimal placement of sensors

A methodology for the optimal sensor locations and multi-scale response reconstruction, which could be possibly used for structural health monitoring and damage detection, was used in this study. Since the structural responses could be reconstructed basing on limited observations, it could also be employed and extended here to improve the robustness and applicability of the aforementioned control system. The minimal number and optimal placement of sensors could be determined with the objective that the reconstructed structural responses can be used as feedbacks for the vibration control while the predetermined control performance can be maintained.

The substitution of Eq. (6) into Eq. (2) yields

$$\{\dot{X}\} = \big[[A_c]-[D_c][G]\big]\{X\}+[B_c]\ddot{x}_g = [A_1]\{X\}+[B_c]\ddot{x}_g \tag{16}$$

For practical consideration, the response measurements of a building structure under earthquake excitation in this study are assumed to be the absolute acceleration responses which can be directly measured by accelerometers. The corresponding observation equation of the controlled building structure can then written as

$$\{Y\} = [C_c]\{X\}+[F_c]\{U\} \tag{17}$$

where $\{Y\}$ denotes the measured absolute acceleration responses of the building structure. $[C_c]$ and $[F_c]$ can be found as follows:

$$[C_c] = \big[-[M]^{-1}[K] \quad -[M]^{-1}[C]\big]; \quad [F_c] = \big[[M]^{-1}[H_c]\big] \tag{18}$$

By using Eq. (6), Eq. (17) can be rewritten as

$$\{Y\} = \big[[C_c]-[F_c][G]\big]\{X\}=[C_1]\{X\} \tag{19}$$

In reality, the measurement data are discretely sampled with a time interval of Δt. Moreover, the measurement noise and process noise always exist in real application. Consequently, the state-space Eq. (16) and the observation Eq. (19) can be converted to the discrete form.

$$\{X\}_{k+1} = [A_2]\{X\}_k+[B_d]\ddot{x}_{g,k}+\{w\}_k \tag{20}$$

$$\{Y\}_k = [C_1]\{X\}_k+\{v\}_k \tag{21}$$

where $\{X\}_{k+1}$ is the discrete state vector; $\{w\}_k$ and $\{v\}_k$ are the process noise and measurement noise, respectively, which are assumed as zero-mean white noise processes with covariance

matrices equal to $[Q_1]$ and $[R_1]$ in this study; $[A_2]$ denotes the discrete-state control matrix; and $[B_d]$ denotes the discrete-state input matrix. They can be expressed as follows

$$\{X\}_k = \{X(k \cdot \Delta t)\} \quad (k=1, 2, 3, \ldots) \tag{22}$$

$$[A_2] = e^{[A_1]\Delta t} ; \quad [B_d] = \int_0^{\Delta t} e^{[A_1]t} dt \cdot [B_c] \tag{23}$$

in which $[A_1]$ and $[B_c]$ are respectively defined in Eq. (16) and Eq. (4).

The Kalman filter provides an unbiased and recursive algorithm to optimally estimate the unknown state vector. It is employed herein for the optimal placement of the sensor as well as the response reconstruction. For the active control of a building structure, the Kalman filter algorithm involves the two sets of equations. The first set of equations is the time update equations

$$\{\hat{X}\}_{k+1|k} = [A_2]\{\hat{X}\}_k + [B_d]\ddot{x}_{g,k} \tag{24}$$

$$[P]_{k+1|k} = [A_2][P]_k[A_2]^T + [Q_1] \tag{25}$$

in which $\{\hat{X}\}_{k+1|k}$ and $[P]_{k+1|k}$ denote a priori state estimate and a priori error covariance matrix, respectively. The second set of equations is the measurement update equations

$$\{\hat{X}\}_{k+1|k+1} = \{\hat{X}\}_{k+1|k} + [K_{KF}]_{k+1}\left\{\{Y\}_{k+1} - [C_1]\{\hat{X}\}_{k+1|k}\right\} \tag{26}$$

$$[P]_{k+1|k+1} = \left[[I] - [K_{KF}]_{k+1}[C_1]\right] \cdot [P]_{k+1|k} \tag{27}$$

$$[K_{KF}]_{k+1} = [P]_{k+1|k}[C_1]^T \cdot \left[[C_1][P]_{k+1|k}[C_1]^T + [R_1]\right]^{-1} \tag{28}$$

in which $\{\hat{X}\}_{k+1|k+1}$ and $[P]_{k+1|k+1}$ are respectively the posterior state estimate and the posterior error covariance matrix; and $[K_{KF}]_{k+1}$ is the optimal Kalman gain matrix.

It is computationally challenging to apply Kalman filter algorithm directly to civil structures with a large number of DOFs involved. Moreover, it is reasonable to assume that under the earthquake excitation, the structural responses are mainly denominated by the first several modes of vibration and the contribution of the modes of vibration with high frequencies could be ignored. In this context, the modal coordinate is employed. Let $\{x\} = [\Phi]_s\{q\}_s$, and the state-space Eq. (2) can then be expressed by

$$\{\dot{Z}\} = [A_c']\{Z\} + [B_c']\ddot{x}_g + [D_c']\{U\} \tag{29}$$

in which

$$\{Z\} = \left[\{q\}_s \quad \{\dot{q}\}_s\right]^T ; \quad \{q\}_s = [q_1 \quad q_2 \quad \ldots \quad q_s]^T \tag{30}$$

$$[A'_c] = \begin{bmatrix} [0] & [I] \\ -[\omega]_s^2 & -2[\xi]_s[\omega]_s \end{bmatrix}; [B'_c] = \begin{bmatrix} \{0\} \\ -[\Phi]_s^T[M]\{1\} \end{bmatrix}; [D'_c] = \begin{bmatrix} [0] \\ [\Phi]_s^T[H_c] \end{bmatrix} \tag{31}$$

where $\{q\}$ is the vector of modal coordinates; subscript s denotes the number of the selected modes of vibration; $[\Phi]_s$ is the selected mass-normalized displacement mode shape matrix; $[\xi]_s$ and $[\omega]_s$ are respectively the modal damping ratio matrix and modal frequency matrix with respect to the selected modes of vibration. In the modal domain, the control force shown in Eq. (6) could be rearranged as

$$\{U\} = -[G]\{X\} = -[G]\begin{bmatrix} [\Phi]_s & [0] \\ [0] & [\Phi]_s \end{bmatrix}\{Z\} \tag{32}$$

Consequently, Eq. (29) can be rewritten as

$$\{\dot{Z}\} = \left[[A'_c] - [D'_c][G]\begin{bmatrix} [\Phi]_s & [0] \\ [0] & [\Phi]_s \end{bmatrix}\right]\{Z\} + [B'_c]\ddot{x}_g = [A'_1]\{Z\} + [B'_c]\ddot{x}_g \tag{33}$$

As mentioned before, the measured responses of the building structure are the absolute accelerations and the observation Eq. (19) can be rewritten as

$$\{Y\} = [C_1]\begin{bmatrix} [\Phi]_s & [0] \\ [0] & [\Phi]_s \end{bmatrix}\{Z\} = [C'_1]\{Z\} \tag{34}$$

To implement the Kalman filter algorithm in the modal domain, the matrices $[A_1]$, $[B_c]$, and $[C_1]$ in Eqs. (20)-(28) should be respectively substituted by $[A_1']$, $[B_c']$, and $[C_1']$ in Eqs. (33) and (34). Furthermore, by comparing Eq. (16) with Eq. (33) one can find that the dimension of the state vectors in the modal domain is significantly reduced. Since the higher-frequency modes which may be falsely excited by noise are truncated in this procedure, it is not only computationally economic but also likely to improve the estimation accuracy to some extent. From this point of view, the modal domain provides a promising way for the use of Kalman filter algorithm in large civil structures.

In this study, the observation equation is used not only to represent the sensor measurement but also to reconstruct the structural responses at unobserved key locations based on the limited accelerometers installed. Therefore, three types of the equations in the discrete forms are introduced according to Eq. (34) as

$$\{Y_e\}_k = [C'_e]\{Z\}_k; \quad \{\hat{Y}_e\}_k = [C'_e]\{\hat{Z}\}_k; \quad \{Y_m\}_k = [C'_m]\{Z\}_k \tag{35}$$

where $\{Y_e\}, \{\hat{Y}_e\}$ and $\{Y_m\}$ represent the real structural responses at the interested locations, the reconstructed structural responses at the interested locations and the measured structural responses from the sensors, respectively; the matrices $[C'_e]$ depends on the locations where the responses are of interest; and $[C'_m]$ depends on the limited number of sensors for measurements.

The accuracy of the reconstructed responses can then be measured by the reconstruction error $\{\delta\}_k$.

$$\{\delta\}_k = \{\hat{Y}_e\}_k - \{Y_e\}_k = [C_e']\left(\{\hat{Z}\}_k - \{Z\}_k\right) \tag{36}$$

Therefore, the asymptotic covariance matrix of the reconstruction error can be expressed as

$$[\Delta] = \mathrm{cov}(\delta) = [C_e'][P][C_e']^T \tag{37}$$

Notably, the output influence matrices $[C_e']$ and $[C_m']$ probably tend to be ill-conditioned or badly scaled especially when only few responses are measured because the absolute acceleration responses of the building structure at different locations may have different orders of magnitude. Without appropriate pre-treatment of the matrix, the inverse operation for the determination of optimal Kalman gain matrix may lead to inaccurate results. Consequently, the standard deviation of the corresponding sensor noise is employed to normalize the matrices $[C_e']$ and $[C_m']$ as

$$[\bar{C}_e'] = [R_e]^{-1/2}[C_e']; \quad [\bar{C}_m'] = [R_m]^{-1/2}[C_m'] \tag{38}$$

where $[R_e]$ and $[R_m]$ are the signal noise matrices with different dimensions. For example, if the measurements are absolute acceleration responses, $[R_m]$ can be expressed as

$$[R_m] = E(vv^T) = \left[[\sigma_a^2][I]\right] \tag{39}$$

in which $[\sigma_a^2]$ is the measurement noise variance matrix of acceleration responses. Hence, the reconstruction error and the corresponding covariance matrix in Eqs. (36) and (37) should be normalized accordingly in consideration of the un-bias estimation.

$$\{\bar{\delta}\}_k = [\bar{C}_e']\left(\{\hat{Z}\}_k - \{Z\}_k\right) \tag{40}$$

$$[\bar{\Delta}] = \mathrm{cov}(\bar{\delta}) = [\bar{C}_e'][P][\bar{C}_e']^T \tag{41}$$

Moreover, since the normalized output influence matrix is used, the optimal Kalman gain shown in Eq. (28) should be updated and given by

$$[K_{\mathrm{KF}}]_{k+1} = [P]_{k+1|k}[\bar{C}_m']^T \cdot \left[[\bar{C}_m'][P]_{k+1|k}[\bar{C}_m']^T + [I]\right]^{-1}[R_m]^{-1/2} \tag{42}$$

It can also be seen that each diagonal element of the $[\bar{\Delta}]$ matrix in Eq. (41) represents the normalized variance of the reconstruction error for the corresponding response. Therefore, the maximum diagonal element denotes the maximum reconstruction error, whereas the trace of the matrix $[\bar{\Delta}]$ represents the sum of the reconstruction errors at all the locations of interest. From this point of view, the optimal sensor placement can be performed with the objective to minimize the sum of the normalized reconstruction error.

$$\text{Object function:} \quad \min \; tr(\bar{\Delta}) \tag{43}$$

$$\text{subject to} \quad \bar{\sigma}_{max} \leq [\sigma_{max}] \tag{44}$$

in which $\bar{\sigma}_{max}$ is the maximum estimation error and defined as

$$\bar{\sigma}_{max} = \max\left(diag(\bar{\Delta})\right) \tag{45}$$

and $[\sigma_{max}]$ is the preset allowable error. It is understood that the maximum value of reconstruction error as well as the trace of the matrix $[\bar{\Delta}]$ would be increased when the number of sensors is reduced. A simple iterative procedure can then be conducted, in which the candidate sensors are removed one by one until the target error level is reached. In each step, only one sensor location, the removal of which leads to a minimal trace of the matrix $[\bar{\Delta}]$, will be deleted. Thus, the sensor with minimal contribution on the response reconstruction will be removed at each step, and this procedure for sensor location is thus suboptimal. Nevertheless, this suboptimal procedure is beneficial and applicable for large-scale and complex structures, for the dimension of the state vectors in the modal domain is significantly reduced when only first several modes are used.

It could be seen that the controlled system with optimal locations of both actuators and sensors can be established according to the approaches presented in Sections 2 and 3, and the schematic diagram is plotted in Fig. 1 for the description of the establishment and application of the determined control system. The number of the control devices and sensors in this control system would be rather small. The feasibility and accuracy of the proposed methodology is investigated in the following section by using a 20-story shear building under earthquake excitation as a numerical example. Moreover, the structural health monitoring and vibration control are expected to be implemented together to form a smart structure in the near future, and the work done in the present study can be therefore considered as the first step towards a smart structure.
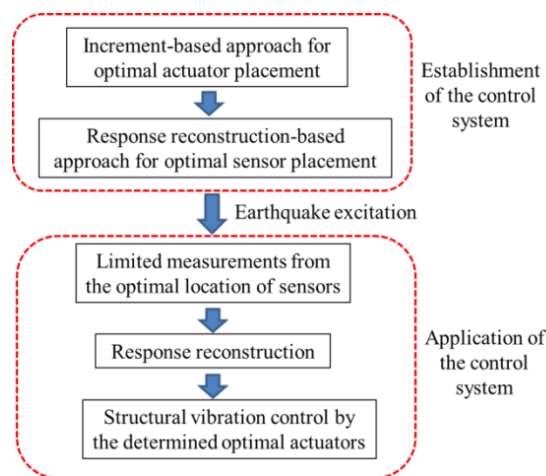
Fig. 1 The schematic diagram for the establishment and application of the proposed control system
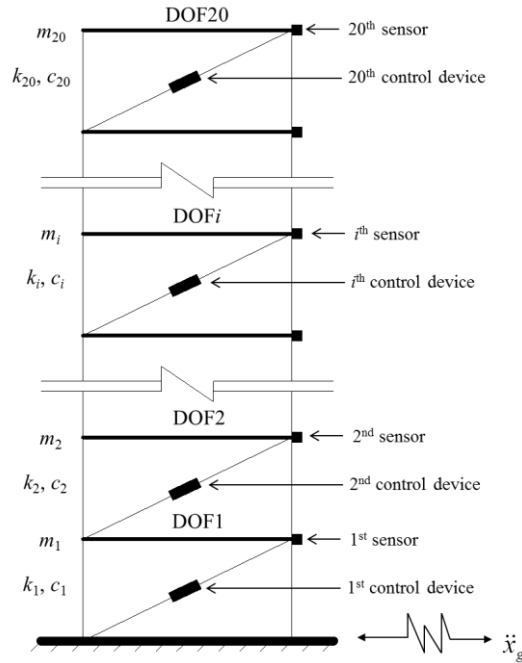
Fig. 2 Structural model of a tall building with control devices and sensors

Table 1 Structural parameters of the 20-story shear building

Floor number	Mass (kg)	Stiffness (N/m)	Floor number	Mass (kg)	Stiffness (N/m)
1-4	8000	9.2×10^7	13-16	8000	7.5×10^7
5-8	8000	8.8×10^7	17-20	8000	7.0×10^7
9-12	8000	8.0×10^7	--	--	--

4. Numerical study

A 20-story shear building as shown in Fig. 2 is employed to investigate the feasibility and accuracy of the proposed method. The mass and stiffness coefficients of the 20-story shear building are listed in Table 1. The Rayleigh damping assumption with the proportional coefficient of 0.8 for the mass matrix and 0.00001 for the stiffness matrix is used to construct the damping matrix. The increment of performance index for vibration control of the building is first computed for the optimal actuator placement. The eigenvalue analysis is then performed to extract the mode shapes for the optimal sensor placement and response reconstruction. The El-Centro ground excitation with a peak acceleration of 0.34 g and the Kobe ground excitation with a peak acceleration of 0.81 g are finally selected as the input to assess the control performance of the building equipped with the selected control system. It should be noted the building model is linear,

and the nonlinear effect on the structural dynamics is not considered and analyzed in this study.

4.1 Determination of the configurations of control system

For the determination of the optimal locations of actuators and sensors, a ground excitation composed of white noise random signals is applied to the shear building. The actuators are initially installed on each floor together with the braces. The weighting matrices $[Q]$ and $[R]$ for the optimal control are selected as follows (Bei and Li 2006)

$$[Q] = \begin{bmatrix} \varphi_1[K] & \varphi_2[M] \\ \varphi_2[M] & \varphi_3[C] \end{bmatrix}; \qquad [R] = \varphi[I] \tag{46}$$

in which $[M]$, $[K]$ and $[C]$ are the mass, stiffness and damping matrix of the shear building, respectively; φ, φ_1, φ_2, and φ_3 are the non-negative number, which are assumed to be $\varphi_1=150$, $\varphi_2=0$, $\varphi_3=350$, and $\varphi=10^{-4}$. By removing the control devices one by one, the increment of performance index is calculated according to Eq. (9) and then the contribution percentage of every controller can be obtained from Eq. (15) as shown in Fig. 3. It can be easily found from Fig. 3 that the sequence of the actuators' locations is 1, 2, 4, 3, 5, 7, 16, 13, 19, 9, 10, 11, 12, 15, 18, 14, 8, 6, 17, and 20. Moreover, the relationship between the summation of *CP* value and displacement reduction on the top floor is given in Fig. 4. It can be seen that with the increase of the summation of *CP* value, the structural responses are reduced accordingly. The dash line indicates the response reduction when twenty actuators are all installed. It can also be found from Fig. 4 that when the summation reaches 70%, the trend for vibration attenuation is becoming slow. Therefore, for the consideration of both effectiveness and economy, the summation of the *CP* value is assumed to be 70% in this study. According to the calculated sequence and the desired summation of the *CP* value, the first ten actuators on the locations of 1, 2, 4, 3, 5, 7, 16, 13, 19, and 9 shall be retained and used for the control.

It is known that in practical situations the structural parameter uncertainties resulting from modeling errors are often existed. Thus, the influence of such uncertainties on the number and location of the actuators is discussed herein. Since it is relatively time-consuming for the consideration of the uncertainties existing in all the structural parameters, only two structural parameters with uncertainties (e.g., k_2 and k_6) are considered for the demonstrative purpose. The values of k_2 and k_6 are approximated as a normal distribution with a mean value of 9.2×10^7 and 8.8×10^7, respectively, and the standard deviation of 5% of the corresponding mean value. Although some variations exist in the calculated *CP* values, for example in some cases CP_{16} becomes larger than CP_7, the aforementioned ten actuators are still retained when the two random parameters are involved. It can thus be concluded, to some extent, from these results that the increment-based approach is not much sensitive to the structural parameter variations.

Furthermore, two integer heuristic programming methods, i.e. the sequential search algorithm (SSA) (Zhang and Soong 1992) and the Worst-Out-Best-In (WOBI) algorithm (Haftkaand Adelman 1985), are employed for determining the optimal actuator location and comparing with the results obtained from the proposed method. For a fair comparison, the control algorithm and weighting matrices used in the SSA and WOBI method are the same as the ones used in the increment-based approach. Then, ten optimal locations out of twenty possible locations will be selected for the placement of the actuators. In this regard, the two performance indices of the building structure are considered. The first one is the maximum peak acceleration on the top floor

described by

$$PI_1 = \max \left\{ | \ddot{x}_{top} | \right\}$$
(47)

The second one is the maximum peak inter-story drift as follows

$$PI_2 = \max \left\{ | \overline{x}_{pi} | \right\} \qquad (i=1, 2,\dots, 20)$$
(48)

in which $| \ddot{x}_{top} |$ and $| \overline{x}_{pi} |$ denotes the absolute value of peak acceleration on the top floor and the absolute value of peak inter-story drift of the *i*-th story, respectively. The objective function to find the optimal location of the actuators is to minimize the maximum peak acceleration response at the top floor (PI_1) and the maximum peak inter-story drift (PI_2), respectively.
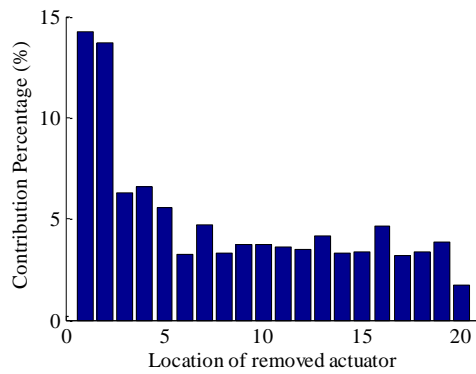
Fig. 3 Optimal sequence of control devices
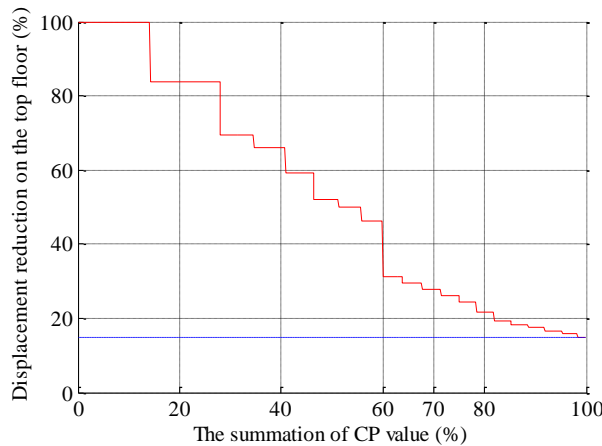
Fig. 4 the relationship between the summation of CP value and displacement reduction

Table 2 The comparison of the actuator locations determined by three algorithms

Algorithm	Objective function	Actuator locations
SSA	*Minimize* (PI_1)	1, 2,4, 5, 7, 9, 10, 13, 15, 20
	Minimize (PI_2)	1,3,5,7,9,13,14,16,18,19
WOBI	*Minimize* (PI_1)	2, 3,5,6,9,10, 13,16,19,20
	Minimize (PI_2)	1,3,5,7,10,13,15,17,19,20
Increment-based approach	*Maximize* (CP)	1, 2, 3, 4, 5,7, 9, 13, 16,19

The actuator locations determined by the SSA and WOBI methods are shown in Table 2. Moreover, the result obtained from the presented increment-based approach is also listed in Table 2. For the sake of easy comparison, the locations are listed in the ascending order. Although there are several different actuator locations, the results obtained by those three algorithms are close to each other. It can also be seen from Table 2 that even for the identical algorithm, the determined actuator locations are not the same if different objective functions are used. It should be noted that for r actuators to be placed in n possible locations, there would be $nr-[r(r-1)/2]$ configurations for SSA and n evaluations of the objective function in each iteration for WOBI. This means that 155 combinations are required to be considered for SSA and 20 location strategies are required to be evaluated in each iteration for WOBI. Moreover, if all of the possible actuator locations are considered, it would be more time-consuming. For example, in our case, i.e., 10 actuators being placed in 20 possible locations, the total number of possible combinations of the actuator locations is $n!/[r!(n-r)!]=20!/(10!\times10!)=184,756$ (Agrawal and Yang 1999).

To determine the optimal placement of the sensors, the approach introduced in Section 3 is employed. The first five modes of vibration with the corresponding natural frequencies of 1.26 Hz, 3.65 Hz, 6.05 Hz, 8.43 Hz and 10.74 Hz are employed. Twenty accelerometers, which are used to measure the acceleration response of each floor, are used as initial candidate locations for sensors. For practical consideration, all the structural response measurements are simulated by the theoretically computed responses superimposed with the white noise with a 5% noise-to-signal ratio in terms of root mean square (RMS). The predefined threshold value of maximum estimation error is applied to determine the number of sensors. It is defined as the ratio of standard deviation of reconstruction error variance to that of noise, which is used to quantify the estimation accuracy. A smaller value of the ratio corresponds to higher estimation accuracy and represents a more stringent criterion on the estimation error, and as a result more sensors are required. It should also be noted if the value of the ratio is too large, the allowable reconstruction error would be too large which may result in the reconstructed responses being probably incorrect or contaminated too much by the noise. In this study, the target maximum estimation error [σ_{max}] in Eq. (44) is set to be 3.0, which means the standard deviation of reconstruction error variance is three times to that of noise. By following the described procedure for the determination of optimal sensor placement, four accelerometers which are respectively located on the 3rd floor, 12th floor, 16th floor, and 20th floor are finally selected. It can be found the number of the sensors is rather reduced as compared with the initial candidate set. Since the locations of the actuators and sensors both are determined, the optimal control system for this shear building is established, which includes ten control devices and four accelerometers. As mentioned before, the standard deviation of the sensor noise is employed to normalize the reconstruction error and the corresponding covariance matrix. It is thus anticipated that the number and location of the selected sensors will be altered if the measurement noise covariance matrix [R_1] is changed. However, in many cases, the measurement noise

covariance is often evaluated prior to the actual operation of the Kalman filter. Thus, for the same sensors under the same conditions, the variation of the measurement noise covariance matrix $[R_1]$ is small and the influence of $[R_1]$ matrix can be controlled in a reasonable range. $[Q_1]$ matrix defined in Eq. (20) is the process noise covariance matrix which is mainly used for the consideration of the modeling errors. The structural parameter uncertainties mentioned before is used herein for briefly investigating the effect of the modeling errors on the optimal sensor placement. Likewise, the values of k_2 and k_6 are approximated as a normal distribution with a mean value of 9.2×10^7 and 8.8×10^7, respectively, and the standard deviation of 5% of the corresponding mean value. With the consideration of these parameter uncertainties, the determined optimal location of the sensors was found to remain unchanged. It should be noted that one basic premise of the presented response reconstruction-based technique is that the structural model is relatively accurate by using the available model updating technique. From this point of view, although the process noise covariance $[Q_1]$ matrix is generally difficult to be estimated, the influence of $[Q_1]$ matrix on the number and location of sensors should be relatively small. Some statements can also be found in Zhang (2012).

4.2 Investigation of the control performance with El-Centro ground excitation

To show the efficiency of the control system with limited actuators and sensors, the El-Centro ground excitation is applied to the shear building with and without the control system. Only the acceleration responses at the 3rd floor, 12th floor, 16th floor and 20th floor of the building are assumed to be measured. The measured responses are then contaminated by 5% white noise. It is noted that although only four acceleration responses are measured, the remaining structural responses can be reconstructed and used for vibration control. Four cases are considered: (1) the actuators and sensors are installed on each floor of the shear building for vibration control (Case 1); (2) the actuators are installed on the determined optimal position (the aforementioned ten locations) but the sensors are installed on each floor of the building for feedback (Case 2); (3) the actuators and sensors both are installed at the determined positions (the aforementioned ten and four positions respectively) and the reconstructed responses are used as feedback for vibration control (Case 3); and (4) no actuators and sensors are installed in the building (without control).

The time histories of acceleration response of the building at the top floor are computed and plotted in Fig. 5 for the four cases. For the sake of clarification, only the time segment of the acceleration responses from 8s to 16s is given in Fig. 5 although the time duration of the displacement response is from 0 to 30s. On one hand, it can be seen that the structural responses of the uncontrolled building are significantly reduced with the control system. On the other hand, the control performance of the optimal control system, defined as Case 3, is close to that of the fully controlled building defined as Case 1. Moreover, it can also be seen that the control performance in Case 3 is in good agreement with that in Case 2, which indicates that the reconstructed responses can be employed for vibration control with acceptable accuracy. Though only the displacement and acceleration responses of the building at the top floor are plotted in Fig. 5, similar results for the remaining building floors can be obtained as well. To have a more comprehensive comparison of the control performance, the maximum displacement and acceleration responses of the building at each floor are depicted in Fig. 6 for the four cases. It can be seen that the maximum responses are significantly reduced when the control devices are employed. It can also be seen that the results of Case 2 and Case 3 are close to each other, implying that the utilization of the reconstructed responses for control is reliable. Though the

maximum displacement and acceleration responses of the building at several upper floors from Case 3 are relatively larger than those from Case 1, the control performance of the optimal control system with only ten actuators and four sensors is still acceptable with consideration of both control-effectiveness and cost-effectiveness.

Moreover, Fig. 7 gives the time histories of the reconstructed displacement and acceleration responses (dashed lines) and the corresponding actual ones (solid lines). Only the displacement and acceleration responses of the building at the top floor are shown in Fig. 7 as an example, and only the time segments from 8 s to 16 s are demonstrated for clarification. It is clear that the reconstructed responses are in good agreement with the corresponding actual responses, confirming that the reconstructed responses could be reliably employed as a feedback for the structural control.

The control performances of the actuator locations determined by SSA and WOBI and shown in Table 2 are also considered herein and compared with those from the presented increment-based approach. The maximum displacement and acceleration responses of the building at each floor are shown in Fig. 8. The cases of the SSA with the objective function of minimizing PI_1 and PI_2 are respectively mentioned as SSA1 and SSA2 in Fig. 8. Similar definition of WOBI1 and WOBI2 can also be found in Fig. 8.
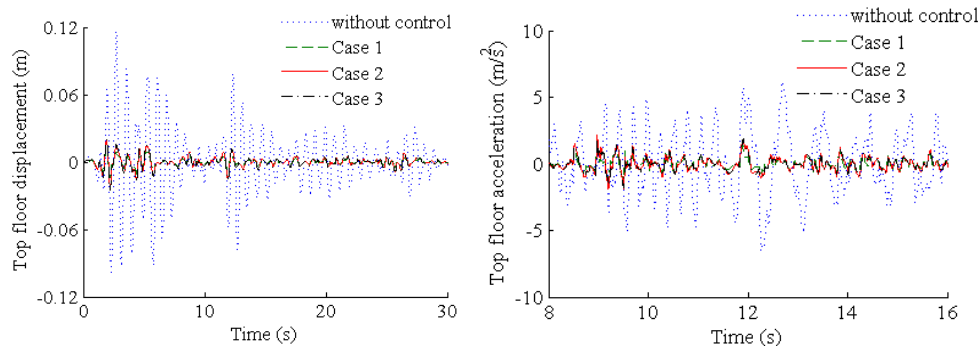
Fig. 5 Time histories of displacement and acceleration responses at the top floor
(El-Centro ground excitation)
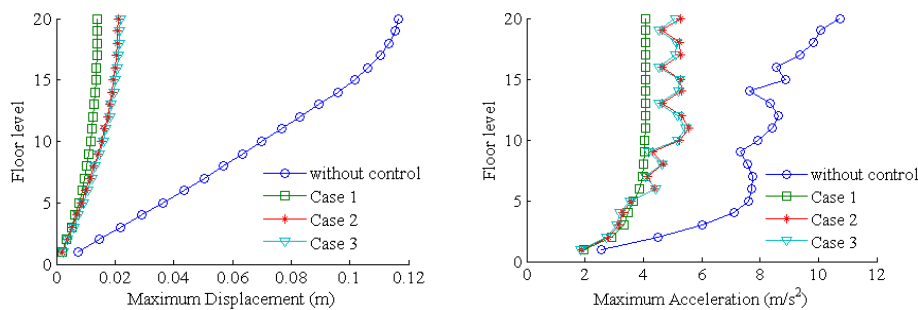
Fig. 6 The comparison of the maximum displacement and acceleration responses
(El-Centro ground excitation)
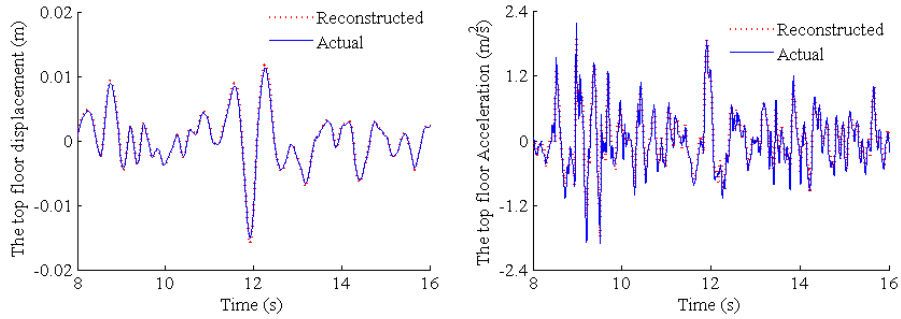
Fig. 7 The comparison of the reconstructed responses with the actual ones (El-Centro ground excitation)
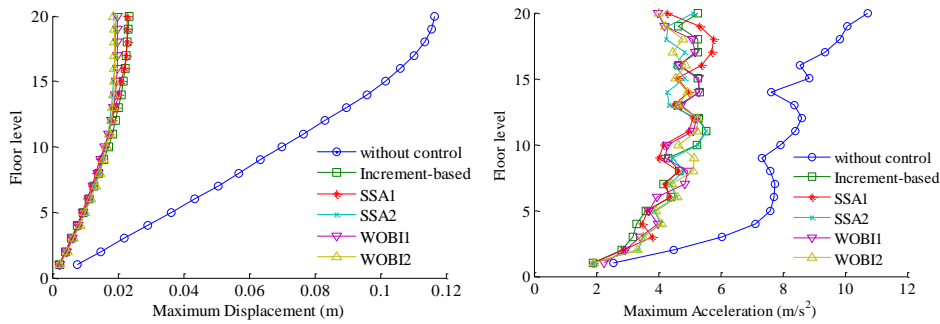
Fig. 8 The comparison of the control performance with different algorithms (El-Centro ground excitation)

It can be seen that although several actuator locations are different according to these algorithms, the control performance is still close to each other. It should also be noted that the complete structural responses, such as the displacement and velocity responses at all floor are assumed to be known for control in SSA and WOBI algorithm whereas only four accelerometers are required in the proposed control system. Moreover, basing on the peak value of the control force, one more performance index is considered and shown as follows (Spencer *et al.* 1998)

$$PI_3 = \left\{ \frac{m\,a\,x\{|U\ t(\}|)}{W} \right\} \tag{49}$$

where $U(t)$ is the control force; and W is the total weight of the building. The values of PI_3 for the aforementioned cases of the full control (i.e., the actuators being installed on each floor of the building), increment-based approach, SSA1, SSA2, WOBI1, and WOBI2 are 0.018, 0.042, 0.044, 0.033, 0.037, and 0.032, respectively. The total energy consumed in the full control, increment-based approach, SSA1, SSA2, WOBI1, and WOBI2 are 1.313×10^4, 1.288×10^4, 1.291×10^4, 1.297×10^4, 1.296×10^4, 1.295×10^4 kN·m, respectively. By comparing with the case of the full control, it can be found that with the reduction of the number of actuators, the control forces of the retained actuators are increasing for the purpose of achieving an acceptable control performance. However, from the viewpoint of the energy consumption, with the identical input energy (e.g. the identical earthquakes applied to the system), the larger extent of system vibration

reduction is achieved, the more energy is consumed by the actuators. Although the control force for each actuator in the case of full control is the smallest, it can be seen that with twenty actuators in this case the total energy consumption is the largest.

4.3 Investigation of the control performance with Kobe ground excitation

To demonstrate the robustness of the optimal control system, the strong Kobe earthquake, which is measured in the near field (the station KJMA) with the epicentral distance of 18.27 km, is applied to the shear building. Similarly, four cases are taken into consideration: (1) the actuators and sensors are installed on each floor of the shear building for vibration control (Case 1); (2) the actuators are installed on the determined optimal position (the aforementioned ten locations) but the sensors are installed on each floor of the building for feedback (Case 2); (3) the actuators and sensors both are installed at the determined positions (the aforementioned ten and four positions respectively) and the reconstructed responses are used as feedback for vibration control (Case 3); and (4) no actuators and sensors are installed in the building (without control). For each case, white noise with 5% noise-to-signal ratio in terms of root mean square (RMS) is superimposed to the numerically-calculated actual structural responses.
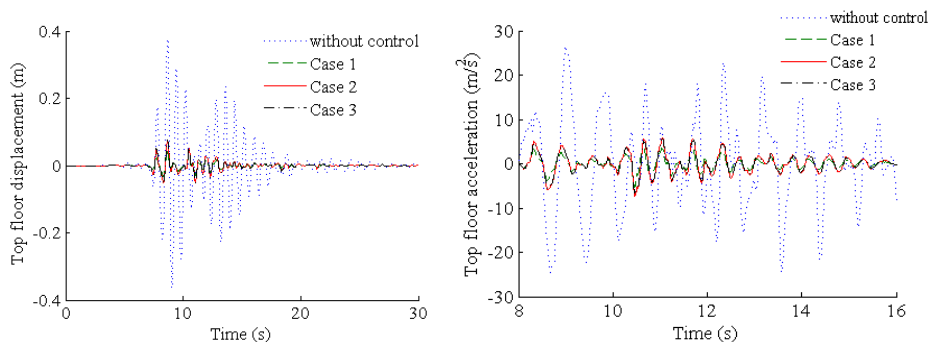
Fig. 9 Time histories of displacement and acceleration responses at the top floor (Kobe ground excitation)
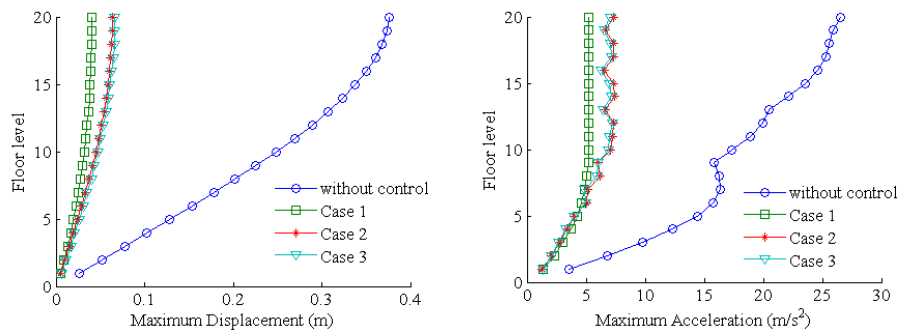
Fig. 10 The comparison of the maximum displacement and acceleration responses (Kobe ground excitation)

    The time histories of the displacement and acceleration responses of the building at the top
floor are shown in Fig. 9 for the four cases. Only the time segments of the acceleration responses
from 8 to 16 s are given in Fig. 9 for the clarification of comparison although the time segments of
the displacement responses are from 0 to 30 s. Moreover, the comparison of the maximum
displacement and acceleration responses of each floor is shown in Fig. 10 for the four cases. It can
be seen from Figs. 9 and 10 that the structural vibration is significantly reduced when the control
devices are employed. It can also be found from these two figures that the response time series as
well as maximum structural responses of the building in Case 3 are rather close to those in Case 2,
implying that the reconstructed responses should be reliable and could be employed as feedback
for vibration control. Though the maximum displacement responses of the building at upper floors
and the maximum acceleration responses of the building at a few floors from Case 3 are relatively
larger than those from Case 1, the control performance of the optimal control system with only ten
actuators and four sensors is still acceptable in consideration of both control-effectiveness and
cost-effectiveness. As a confirmation, the time histories of the reconstructed acceleration and
displacement responses of the building at the top floor are compared with the actual structural
responses and the comparative results are shown in Fig. 11. It is clear that the reconstructed
responses are close to the actual ones. Similar results can be obtained for the rest of building
floors.
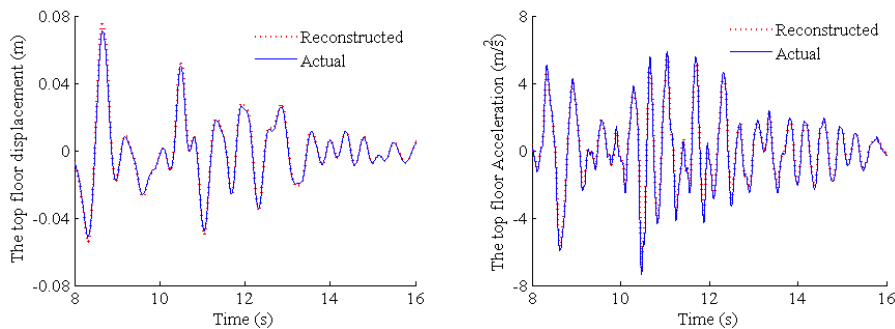
Fig. 11 The comparison of the reconstructed responses with the actual ones (Kobe ground excitation)
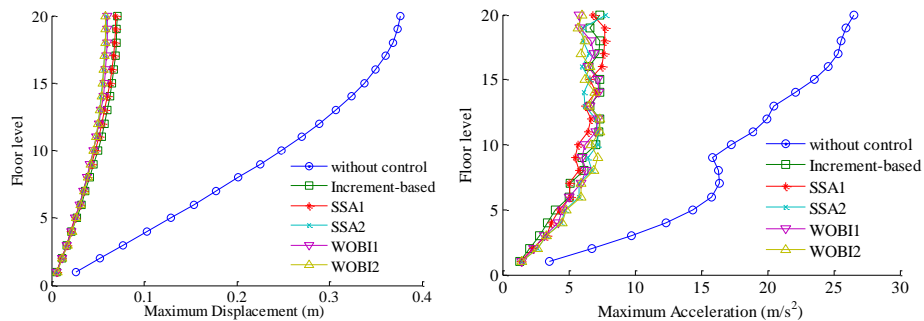
Fig. 12 The comparison of the control performance with different algorithms (Kobe ground excitation)

Table 3 The control performance of the system under other earthquakes

Approaches for actuator locations	Northridge earthquake				Hachinohe earthquake			
	PI_1 (m/s^2)	PI_2 (mm)	PI_3	Total energy consumption (kN·m)	PI_1 (m/s^2)	PI_2 (mm)	PI_3	Total energy consumption (kN·m)
Without control	4.227	2.854	--	--	15.51	14.467	--	--
Full control	1.515	0.711	0.007	6.556×10^2	3.08	3.207	0.026	2.775×10^4
Increment-based	1.977	0.942	0.017	6.364×10^2	4.96	5.267	0.053	2.706×10^4
SSA1	1.759	0.926	0.018	6.388×10^2	4.47	4.904	0.054	2.715×10^4
SSA2	1.932	0.878	0.014	6.415×10^2	4.68	4.494	0.047	2.727×10^4
WOBI1	1.719	0.901	0.016	6.412×10^2	4.32	4.769	0.051	2.726×10^4
WOBI2	1.805	0.859	0.013	6.406×10^2	4.55	4.335	0.048	2.725×10^4

Moreover, the comparison of control performance among the SSA and WOBI methods and the presented increment-based approach is also considered herein and the results are shown in Fig. 12. As mentioned before, the SSA and WOBI with the objective function of minimizing PI_1 and PI_2 are respectively mentioned as SSA1, SSA2, WOBI1, and WOBI2. It could be seen that the results obtained from these three algorithms are close to each other. Furthermore, the index PI_3 defined in Eq. (49) is also investigated herein. The corresponding values for the full control, increment-based approach, SSA1, SSA2, WOBI1, and WOBI2 are 0.043, 0.084, 0.088, 0.079, 0.082, and 0.075, respectively. It can be derived that, even under the Kobe ground excitation with a peak acceleration of 0.81g, the maximum control force is around 140 kN which would be probably realized by many hydraulic actuators. Moreover, the total energy consumed in the full control, increment-based approach, SSA1, SSA2, WOBI1, and WOBI2 are 8.931×10^4, 8.783×10^4, 8.801×10^4, 8.832×10^4, 8.827×10^4, 8.828×10^4 kN·m, respectively. It can be found that the total energy consumption in the case of full control is largest whereas the energy consumption in the proposed approach is the smallest.

Two more ground excitations, i.e., Northridge earthquake with a peak acceleration of 0.15 g and Hachinohe earthquake with a peak acceleration of 0.55 g, are considered for further investigation of robustness of the control system. The corresponding results are given in Table 3. It can be found that the control performance of the proposed approach is close to SSA and WOBI method. Although better control performance can be achieved in the case of the full control, the corresponding total energy consumption and the number of actuators in this case are the largest. Furthermore, the purchase, installation and maintenance of twenty actuators in the full control would be much more expensive than the case of only ten actuators involved in the proposed control system. From these points of view, it can be concluded the presented approach is relatively cost-effective in terms of both energy consumption and less number of actuators.

5. Conclusions

A relatively simple and cost-effective method has been presented in this paper for the determination of the minimal number and optimal location of actuators and sensors for vibration control of building structures under earthquake excitation. The optimal location of the actuator is first determined according to the presented increment-based approach with few iterations, for example, in the 20 DOFs shear building structures, the values of *CP* are only calculated for 20 times. Moreover, in many previous studies the complete response measurements are required for the vibration control after the locations and numbers of the actuators are determined. This requirement will significantly hamper the application of the control system to real civil structures. To overcome this problem, this study extends the response reconstruction-based approach to determine optimal sensor placement and at the same time reconstructing structural responses for vibration control. The work done in this study could also be considered as the first step towards a smart structure in which the structural health monitoring and vibration control shall be implemented together. The feasibility and accuracy of the optimal control system determined by the proposed method has been investigated through a 20-story shear building under the El-Centro and Kobe ground excitations. The numerical results show that although the number of the actuators and sensors are significantly reduced, the control performance achieved by the optimal control system is still close to that by the fully control system. By comparing the reconstructed responses with the actual ones, it shows that the reconstructed information is in good agreement with the real one and can be used for vibration control.

To further investigate the efficiency of the proposed control system, two integer heuristic programming methods (the sequential search algorithm (SSA) and the Worst-Out-Best-In (WOBI) algorithm) have been employed to determine the optimal location of actuators and the corresponding results have been compared with those of the proposed control system. It has been found from the comparative results that only small actuator locations are different and the control performances of the three methods are close to each other. However, as compared with the SSA and WOBI methods, the present method for the determination of the actuator locations is not time consuming because only fewer iterations are required. Furthermore, in the proposed control system both the actuators and sensors are reduced, which are more feasible and applicable to real civil structures compared with other control schemes.

Acknowledgements

References

Agrawal, A.K. and Yang, J.N. (1999), "Optimal placement of passive dampers on seismic and wind-excited buildings using combinatorial optimization", *J. Intel. Mat. Syst. Str.*, **10**(12), 997-1014.
Aupérin, M., Dumoulin, C., Magonette, G.E., Marazzi, F., Försterling, H., Bonefeld, R., Hooper, A. and Jenner, A.G. (2001), "Active control in civil engineering: from conception to full scale applications",

Struct. Control Health Monit., **8**(2), 123-178.

Aydin, E., Boduroglu, M.H. and Guney, D. (2007), "Optimal damper distribution for seismic rehabilitation of planar building structures", *Eng. Struct.*, **29**(2), 176-185.

Barthorpe, R.J. and Worden, K. (2009), "Sensor placement optimization", *Encyclopedia Struct. Health Monit.*, **3**, 1239-1250.

Bei, W.M. and Li, H.N. (2006), "Optimal placement of semi-active control devices for controlled structure", *J. Disaster Prev. Mitigation Eng.*, **26**(1), 28-33.

Bigdelia, K., Hareb, W. and Tesfamariam, S. (2012), "Configuration optimization of dampers for adjacent buildings under seismic excitations", *Eng. Optimiz.*, **44**(12), 1491-1509.

Fisco, N.R. and Adeli, H. (2011), "Smart structures: Part I—active and semi-active control", *ScientiaIranica*, **18**(3), 275-284.

Frecker, M.I. (2003), "Recent Advances in optimization of smart structures and actuators", *J. Intel. Mat. Syst. Str.*, **14**(4-5), 207-216.

Gupta, V., Sharma, M. and Thakur, N. (2010), "Optimization criteria for optimal placement of piezoelectric sensors and actuators on a smart structure: a technical review", *J. Intel. Mat. Syst. Str.*, **21**(12), 1227-1243.

Hac, A. and Liu, L. (1993), "Sensor and actuator location in motion control of flexible structures", *J. Sound Vib.*, **167**(2), 239-261.

Haftka, R.T. and Adelman, H.M. (1985), "Selection of actuator locations for static shape control of large space structures by heuristic integer programming", *Comput. Struct.*, **20**(1-3), 578-582.

Heo, G., Wang, M.L. and Satpathi, D. (1997), "Optimal transducer placement for health monitoring of long span bridge", *Soil Dyn. Earthq. Eng.*, **16**(7-8), 495-502.

Housner, G., Bergman, L., Caughey, T., Chassiakos, A., Claus, R., Masri, S.F., Skelton, R., Soong, T.T., Spencer Jr, B.F. and Yao, J. (1997), "Structural control: past, present, and future", *J. Eng. Mech. - ASCE*, **123**(9), 897-971.

Ikeda, Y. (2009), "Active and semi-active vibration control of buildings in Japan—Practical applications and verification", *Struct. Control Health Monit.*, **16**(7-8), 703-723.

Kammer, D.C. (1991), "Sensor placement for on-orbit modal identification and correlation of large space structures", *J. Guid. Control Dynam.*, **14**(2), 251-259.

Li, D.S., Li, H.N. and Fritzen, C.P. (2007), "The connection between effective independence and modal kinetic energy methods for sensor placement", *J. Sound Vib.*, **305**(4-5), 945-955.

Liu, W., Tong, M. and Lee, G.C. (2005), "Optimization methodology for damper configuration based on building performance indices", *J. Struct. Eng. - ASCE*, **131**(11), 1746-1756.

Peng, F.J., Ng, A. and Hu, Y.R. (2005), "Actuator placement optimization and adaptive vibration control of plate smart structures", *J. Intel. Mat. Syst. Str.*, **16**(3), 263-271.

Rao, A.R.M. and Anandakumar, G. (2008), "Optimal sensor placement techniques for system identification and health monitoring of civil structures", *Smart Struct. Syst.*, **4**(4), 465-492.

Soong, T.T. and Spencer Jr., B.F. (2002), "Supplemental energy dissipation: state-of-the-art and state-of-the-practice", *Eng. Struct.*, **24**(3), 243-259.

Spencer Jr., B.F., Dyke, S.J. and Deoskar, H.S. (1998), "Benchmark problems in structural control: part II-active tendon system", *Earthq. Eng. Struct. D.*, **27**(11), 1141-1147.

Spencer Jr., B.F. and Nagarajaiah, S. (2003), "State of the art of structural control", *J. Struct. Eng. - ASCE*, **129**(7), 845-856.

Takewaki, I. (1997), "Optimal damper placement for minimum transfer function", *Earthq. Eng. Struct. D.*, **26**(11), 1113-1124.

Takewaki, I. (2000), "Optimum damper placement for planar building frames using transfer functions", *Struct. Multidiscip. O.*, **20**(4), 280-287.

Udwadia, F.E. (1994), "Methodology for optimum sensor locations for parameter identification in dynamic system", *J. Eng. Mech. - ASCE*, **120**(2), 368-390.

Whittle, J.K., Williams, M.S., Karavasilis, T.L. and Blakeborough, A. (2012), "A comparison of viscous damper placement methods for improving seismic building design", *J. Earthq. Eng.*, **16**(4), 540-560.

Xu, Y.L. and Teng, J. (2002), "Optimum design of active/passive control devices for tall buildings under

earthquake excitation", *Struct. Des. Tall Build.*, **11**(2), 109-127.

Xu, Y.L. and Ng, C.L. (2008), "Seismic protection of a building complex using variable friction damper: Experimental investigation", *J. Eng. Mech. - ASCE*, **134**(8), 637-649.

Yi, T.H., Li, H.N. and Gu, M. (2012), "Sensor placement for structural health monitoring of Canton Tower", *Smart Struct. Syst.*, **10**(4), 313-329.

Zhang, R.H. and Soong, T.T. (1992), "Seismic design of viscoelastic dampers for structural applications", *J. Struct. Eng. - ASCE*, **118**(5), 1375-1392.

Zhang, X.H., Zhu, S., Xu, Y.L. and Hong, X.J. (2011), "Integrated optimal placement of displacement transducers and strain gauges for better estimation of structural response", *Int. J. Struct. Stab Dyn.*, **11**(3), 581-602.

Zhang, X.H. (2012), *Multi-sensing and multi-scale monitoring of long-span suspension bridges*, PhD thesis, Department of Civil and Environmental Engineering, Ph.D. Dissertation, The Hong Kong Polytechnic University, Hong Kong.

CY